Open access • Journal Article • DOI:10.1063/1.126989

Minority carrier diffusion, defects, and localization in InGaAsN with 2% nitrogen

Steven R. Kurtz, Andrew A. Allerman, C. H. Seager, R. M. Sieg ...+1 more authors

Published on: 07 Jul 2000 - Applied Physics Letters (American Institute of Physics)

Topics: Carrier lifetime, Electron mobility and Hall effect

SAND2000-1115J

Minority Carrier Diffusion, Defects, and Localization in InGaAsN, with 2% Nitrogen

Steven R. Kurtz, A. A. Allerman, C. H. Seager , R. M. Sieg, and E. D. Jones

Sandia National Laboratories

Albuquerque, NM 87185-0603

Electron and hole transport in compensated, InGaAsN (≈ 2% N) are examined through Hall mobility, photoconductivity, and solar cell photoresponse measurements. Short minority carrier diffusion lengths, photoconductive-response spectra, and doping dependent, thermally activated Hall mobilities reveal a broad distribution of localized states. At this stage of development, lateral carrier transport appears to be limited by large scale (>> mean free path) material inhomogeneities, not a random alloy-induced mobility edge.

DISCLAIMER

DISCLAIMER

Portions of this document may be illegible in electronic image products. Images are produced from the best available original document.

InGaAsN alloys are being developed as long wavelength materials for laser and multi-junction solar cell applications. Bandgaps of ≤ 1.0 eV are obtained for $In_xGa_{1-x}As_{1-y}N_y$ with minimal N concentrations ($y \geq 0.02$), and the quaternary is lattice-matched to GaAs for compositions with $x \approx 3y$.[1-3] Even at these low concentrations, N incorporation has proven problematic, and device performance has not reached expectations, with radiative efficiencies [4] and minority carrier diffusion lengths [5] diminishing with increasing N concentration. Supercell bandstructure calculations for InGaAsN indicate that introduction of N leaves the valence band GaAs-like, but N distorts the conduction band through symmetry-breaking and altered charge densities.[6-9] Introducing disorder into the picture, with the N atoms producing random alloy fluctuations, leads to speculation that N incorporation may result in intrinsic localization and a mobility-edge which would degrade device performance. Since bandstructure calculations predict that N strongly perturbs the conduction band, electrons should be most affected by the N-induced fluctuations. In this paper, we examine electron and hole transport in InGaAsN through Hall mobility, photoconductivity, and solar cell photoresponse measurements. Our observations suggest that lateral carrier transport is presently limited by InGaAsN material inhomogeneities, not a random alloy-induced mobility-edge.

Samples used in this work were grown by metalorganic chemical vapor deposition, using trimethylindium, trimethylgallium, 100% arsine, and dimethylhydrazine sources. N-type material was achieved using tetraethyltin doping. The composition was determined by calibration growths of GaAsN and InGaAs along with double crystal x-ray diffraction measurements, and all samples are nominally lattice matched to their GaAs substrates. Samples described in this work were annealed at 650°C for 30 minutes.[4,5] In our high quality InGaAsN, we find that annealing increases minority carrier diffusion lengths and background acceptor concentrations.

Minority carrier devices are very sensitive to localization and trapping. To determine the effect of N on electron and hole diffusion lengths, we compared structurally similar solar cells, with different InGaAsN compositions. Our non-optimized, test-cell consisted of a thick (1 μm) n-type InGaAsN base, a thin (0.2-0.3 μm) p-type InGaAsN emitter, an p-type (500 Å) AlGaAs window, and a GaAs contact (p-type, 300 Å). These cells were grown on n-type, GaAs substrates. Internal quantum efficiency (IQE) measurements for InGaAsN solar cells with 1.0 eV and 1.1 eV bandgap InGaAsN (2.1% and 1.1% N, respectively) are shown in Figure 1. From absorption data and layer thickness, IQEs were simulated to determine minority carrier diffusion lengths in each of the InGaAsN layers. In the emitter of the 1.0 eV InGaAsN cell, electrons are localized, with a diffusion length $\approx 10^{-2}$ μm, and in the 1.1 eV InGaAsN emitter, electron diffusion has increased to 0.2 μm. In both cells, a hole diffusion length of ≈ 1 μm is obtained for the base layer. Open circuit voltages, at air-mass 0, for the 1.0 eV and 1.1 eV cells are 0.41 and 0.50 V, respectively. Although these values are near state-of-the-art for InGaAsN solar cells, short carrier diffusion lengths (particularly electrons) limit InGaAsN bipolar device performance.

Alloy scattering rates for electrons should be greater for GaAsXN (X= In, P, Sb, Al...) than other III-V alloys. GaAsXN conduction band fluctuations are proportional to the differences in electronegativity [10] between the binary constituents (GaAs (2.9 eV) vs GaN (7.6 eV))[11] or alternatively, to the variation of conduction band energy with composition .[12] Depending on the value used for the energy fluctuations, one calculates a conduction band mobility for InGaAsN (2 % N) at 300 K in the range 100-500 $cm^2/V.s$, limited by alloy scattering.[10] Hall mobility measurements were made on a series of compensated InGaAsN samples with nominally the same composition ,1.6-1.9% N. N-type (Sn) doping levels were varied in this series to range from as-grown p-type to n-type,mid-$10^{17}/cm^3$. At 300 K and high carrier densities, the electron mobility curves in Fig. 2(a) converge to ≈ 300 $cm^2/V.s$, consistent with the upper limit imposed by alloy scattering.[13] Hole mobilities (Fig. 2(b)) at 300 K ranged even lower, 60-90 $cm^2/V.s$.

Hall mobility measurements were made on the InGaAsN films versus temperature and doping. Electron mobility (Fig. 2(a)) is thermally activated near 300 K and becomes weakly temperature dependent at low temperatures These activation energies increase with decreasing electron concentration, ranging from 42 meV @ $2x10^{16}$ e/cm^3 to 0 meV @ $6x10^{17}$ e/cm^3. Based on limited data, we find that hole mobilities are qualitatively similar to those observed for the electrons. For both electrons and holes, the carrier concentration was only weakly temperature dependent over the range 15-300 K. At the lowest carrier concentrations and temperatures, some Hall data were not reported due to large asymmetries of the van der Pauw resistances and inconsistent Hall data obtained upon field reversal. Surface potential profile measurements reveal resistivity gradients of $\approx$ 2x/cm in those samples displaying the largest van der Pauw asymetries.[14]

Overall, these Hall data are inconsistent with an electron mobility-edge because: 1) Our Hall mobilities, not carrier concentrations, are thermally activated; 2) Holes display similar behavior to electrons; and 3) Low temperature mobility values are large for variable-range hopping.[15] Instead, we believe that InGaAsN carrier transport is modulated by large scale (i.e. >> mean free path) inhomomgeneities, forming potential barriers. Consistent with our data, the Hall mobility is thermally activated in such inhomogeneous materials,[16] and Hall data for polycrystalline Si are strikingly similar to our InGaAsN results.[17] Increased n-type doping lowers Hall mobility activation energy by approximately the increase in Fermi energy. Among the numerous possible explanations, phase-separation-induced inhomogeneities in N concentration ($\geq$ 0.25 %) would produce such barriers, or long range dopant variations could give rise to regions where the compensation of the native p-type dopant varies considerably. Inhomogeneities have not yet been observed with transmission electron microscopy, but preliminary scanning-tunneling-microscopy images of our material indicate $\approx$ 200 Å features.[18]

With photoconductivity and photoluminescence spectroscopies, we studied the same samples used for Hall measurements. We found that lightly doped, n-type samples

luminesce at significantly lower energy and intensity than more heavily doped samples in the series (see Fig. 3(a)). Photoconductivity will be largest for photon energies above the energies of barriers limiting the Hall mobilities, and the band-edge features in the photoconductivity spectra (see Fig. 3(b)) for all samples occur at ≈ 1.14 eV (@ 77K), in better agreement with the photoluminescence peaks observed in the heavily doped samples. We estimate the n-type, $9x10^{16}/cm^3$ InGaAsN photoluminescence peak is ≈ 100 meV lower in energy than the photoconductivity band-edge. (In the p-type, $5x10^{16}/cm^3$ sample the energy difference was ≤ 50 meV, near the limit of our resolution.) The resolved energy shift between the photoluminescence peak and photoconductivity band-edge feature indicates that electrons are localized at low temperature in the lightly doped n-type ($\leq 9x10^{16}/cm^3$) InGaAsN. Recent, time-resolved photoluminescence studies of annealed InGaAsN quantum wells also indicate a distribution of localized states near the band-edge.[19]

Sub-bandgap features are clearly observed throughout the photoconductivity and photoluminescence spectra. In the photoconductive response (Fig. 3(b)), an "Urbach tail" [15] appears below the band-edge in the 0.8-1.1 eV range, and a corresponding, broad photoluminescence feature (Fig. 3(a)) is observed throughout that range. Photoconductive response indicates the presence of a mid-gap, ≈ 0.6-0.8 eV, feature which seems to occur with Sn doping. We believe the mid-gap state is associated with a dopant-related impurity, not the Sn-donor level.

In summary, we have investigated carrier transport in InGaAsN (≈ 2% N) using several techniques. Electron minority carrier diffusion is minimal, and both electron and hole transport may be limited by large-scale inhomogeneities, similar to behavior observed in polycrystalline Si. Photoconductivity and photoluminescence reveal a broad distribution of sub-bandgap states in both n and p-type InGaAsN. Clearly, further studies of InGaAsN, grown under different conditions, are required before we can assign "intrinsic" transport properties and limitations to this intriguing material.

The authors thank J. A. Bur and T. Hargett for technical support. Sandia is a multiprogram laboratory operated by Sandia Corporation, a Lockheed Martin Company, for the U.S. Dept. of Energy under contract DE-AC04-94AL85000. Additional funding was provided by Air Force Research Laboratory and Lockheed Martin.

Figure Captions –

Figure 1 – Spectral response of two InGaAsN cells with different alloy compositions (1% and 2% N). Cell simulations (dashed lines) and respective electron (L_n) and hole (L_p) minority carrier diffusion lengths are indicated in the figure.

Figure 2 – Hall mobility versus temperature for a series of n (a) and p-type (b), InGaAsN samples doped at different levels. Thermal activation energies (E_A) are indicated in the figure.

Figure 3 – Photoluminescence (a) and photoconductivity (b) spectra (77 K) for InGaAsN samples doped at different levels. Approx. photoconductive bandgap energy is indicated by the vertical lines.

REFERENCES

1. M. Weyers, M. Sato, and H. Ando, Jpn. J. Appl Phys. 31, 853 (1992).
2. S. Sato, Y. Osawa, and T. Saitoh, Jpn. J. Appl. Phys. 36, 2671 (1997).
3. M. Kondow, T. Kitatani, S. Nakatsuka, M. C. Larson, K. Nakahara, Y. Yazawa, and M. Okai, IEEE J. of Selected Topics in Quant. Elect. 3, 719 (1997).
4. E. V. K. Rao, A. Ougazzaden, Y. Le Bellego, and M. Juhel, Appl . Phys. Lett. 72, 1409 (1998).
5. Steven R. Kurtz, A. A. Allerman, E. D. Jones, J. M. Gee, J. J. Banas, and B. E. Hammons, Appl. Phys. Lett. 74, 729 (1999).
6. L. Bellaiche, S.-H. Wei, and Alex Zunger, Phys. Rev. B 54, 17568 (1996), and T. Mattila, S.-H. Wei, and Alex Zunger, Phys. Rev. B 60, 11245 (1999).
7. J. D. Perkins, A. Mascarenhas, Y. Zhang, J. F. Geisz, D. J. Friedman, J. M. Olsen, and S. R. Kurtz, Phys. Rev Lett. 82, 3312 (1999).
8. W. Shan, W. Walukiewicz, J. W. Ager III, E. E. Haller, J. F. Geisz, D. J. Friedman, J. M. Olsen, and S. R. Kurtz, Phys. Rev. Lett. 82, 1221 (1999).
9. E. D. Jones, N. A. Modine, A. A. Allerman, S. R. Kurtz, A. F. Wright, S. T. Tozer, and X. Wei, Phys. Rev. B 60, 4430 (1999).
10. J. W. Harrison and J. R. Hauser, Phys. Rev. B 13, 5347 (1976).
11. J. A. Van Vechten Phys. Rev. 187, 1007 (1969).
12. M. Auslander and S. Hava, Solid State Commun. 87, 335 (1993).
13. C. Skierbiszewski, P. Perlin, P. Wisniewski, T. Suski, W. Walukiewicz, W. Shan, J. W. Ager, E. E. Haller, J. F. Geisz, D. J. Friedman, J. M. Olsen, and S. R. Kurtz, Phys. Stat. Sol.(b) 216, 135 (1999).
14. Steven R. Kurtz, C. H. Seager, A. A. Allerman, R. M. Sieg, and E. D. Jones, to be published.

15. N. F. Mott and E. A. Davis, Electronic Processes in Non-Crystalline Materials, 2nd Ed., Clarendon Press, Oxford, 1979

16. V. G. Karpov, A. Ya. Shik, and B. I. Shklovski, Sov. Phys. Semi. 16, 901 (1982).

17. H. Paul Maruska, Amal K. Ghosh, Albert Rose, and Tom Feng, Appl. Phys. Lett. 36, 381 (1980).

18. H. K. Lyeo, C. K. Shih, A. A. Allerman, S. R. Kurtz, and E. D. Jones, to be published.

19. R. A. Mair, J. Y. Lin, H. X. Jiang, E. D. Jones, A. A. Allerman, and S. R. Kurtz, Appl. Phys. Lett. 76, 188 (1999).

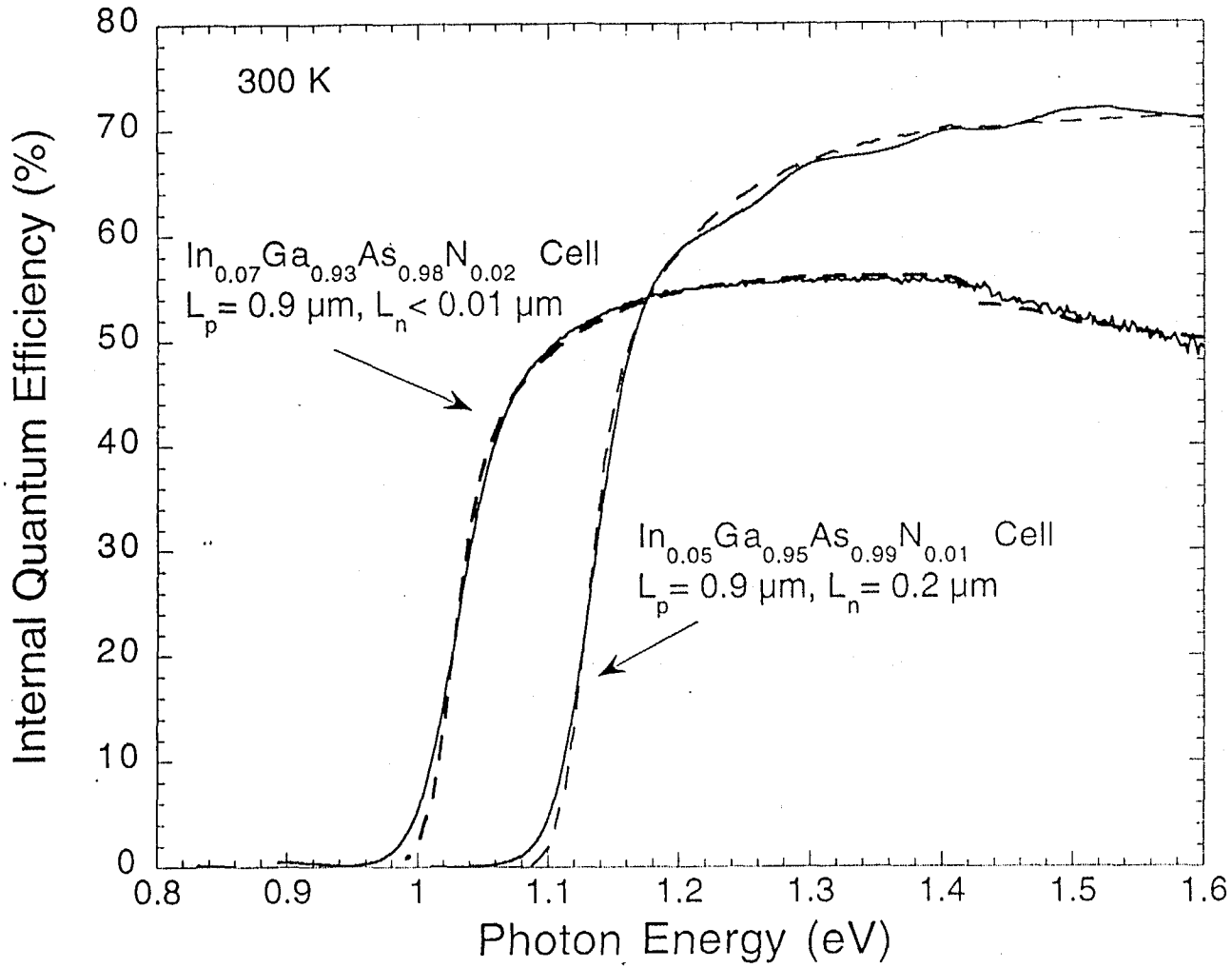
300 K
$In_{0.07}Ga_{0.93}As_{0.98}N_{0.02}$ Cell
L_p = 0.9 μm, L_n < 0.01 μm
$In_{0.05}Ga_{0.95}As_{0.99}N_{0.01}$ Cell
L_p = 0.9 μm, L_n = 0.2 μm
Internal Quantum Efficiency (%)
Photon Energy (eV)
0
10
20
30
40
50
60
70
80
0.8
0.9
1
1.1
1.2
1.3
1.4
1.5
1.6

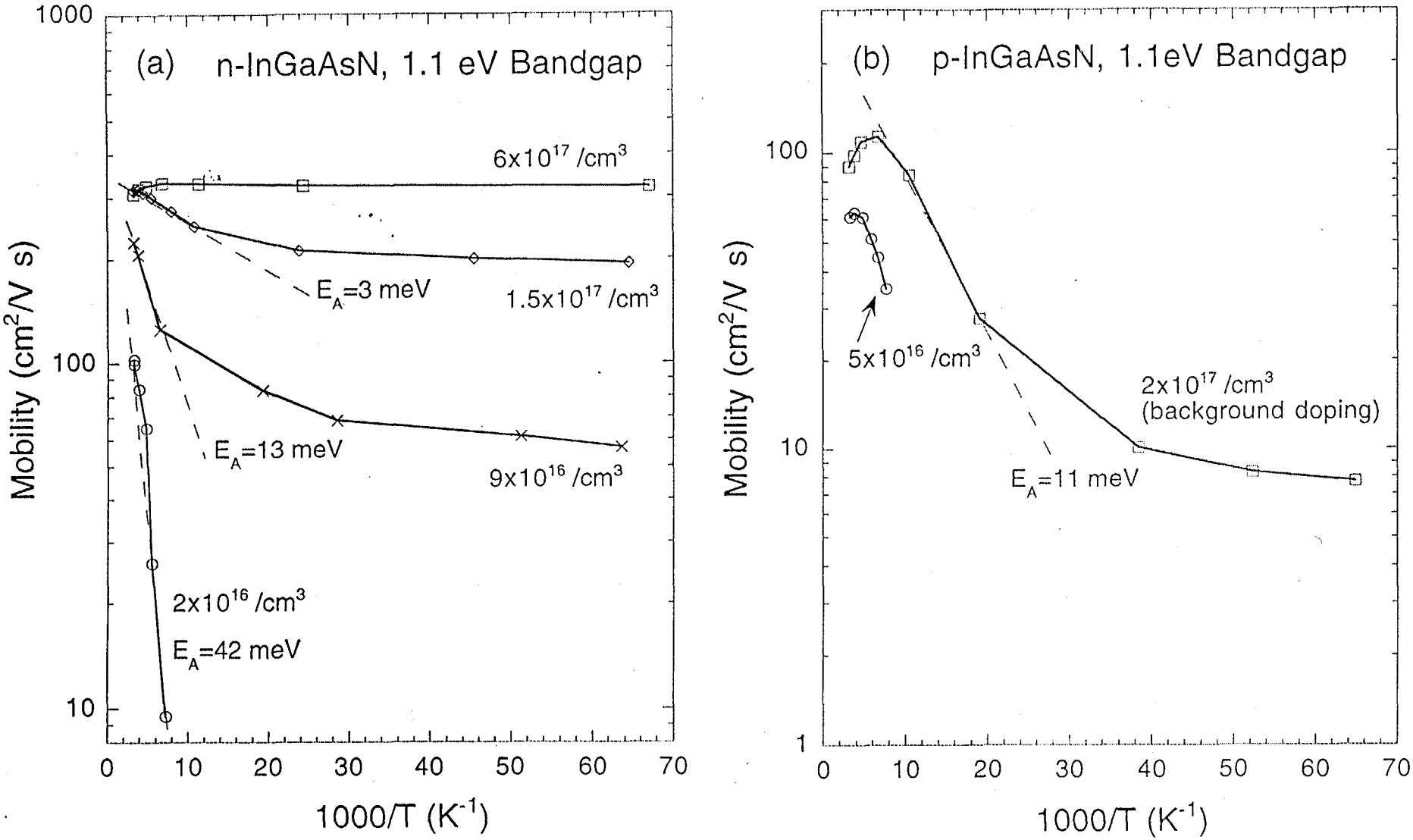
(a) n-InGaAsN, 1.1 eV Bandgap
6x10^17 /cm^3
1.5x10^17 /cm^3
E_A=3 meV
E_A=13 meV
9x10^16 /cm^3
2x10^16 /cm^3
E_A=42 meV
Mobility (cm^2/V s)
1000/T (K^-1)
1000
100
10
0
10
20
30
40
50
60
70
(b) p-InGaAsN, 1.1eV Bandgap
5x10^16 /cm^3
2x10^17 /cm^3
(background doping)
E_A=11 meV
Mobility (cm^2/V s)
1000/T (K^-1)
100
10
1
0
10
20
30
40
50
60
70

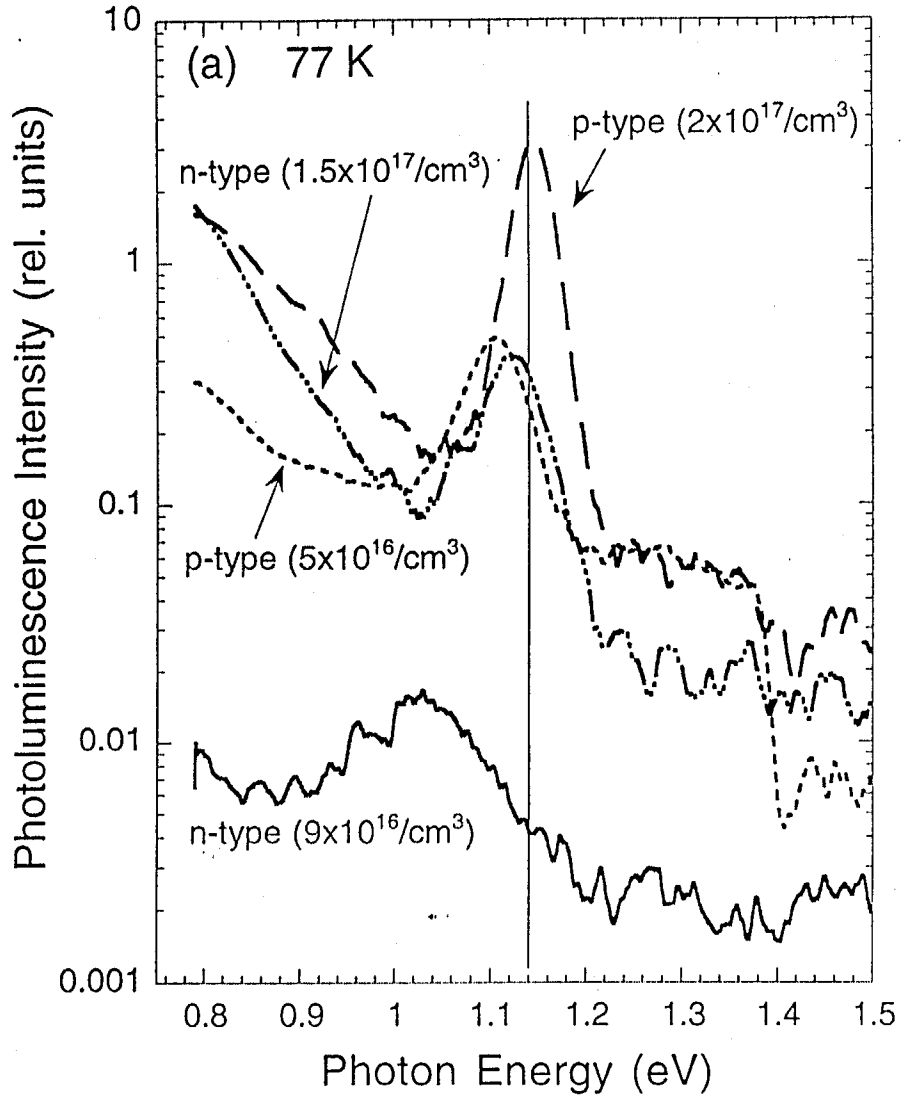
(a) 77 K
n-type (1.5x10^17/cm^3)
p-type (2x10^17/cm^3)
p-type (5x10^16/cm^3)
n-type (9x10^16/cm^3)
Photoluminescence Intensity (rel. units)
Photon Energy (eV)
10
1
0.1
0.01
0.001
0.8
0.9
1
1.1
1.2
1.3
1.4
1.5

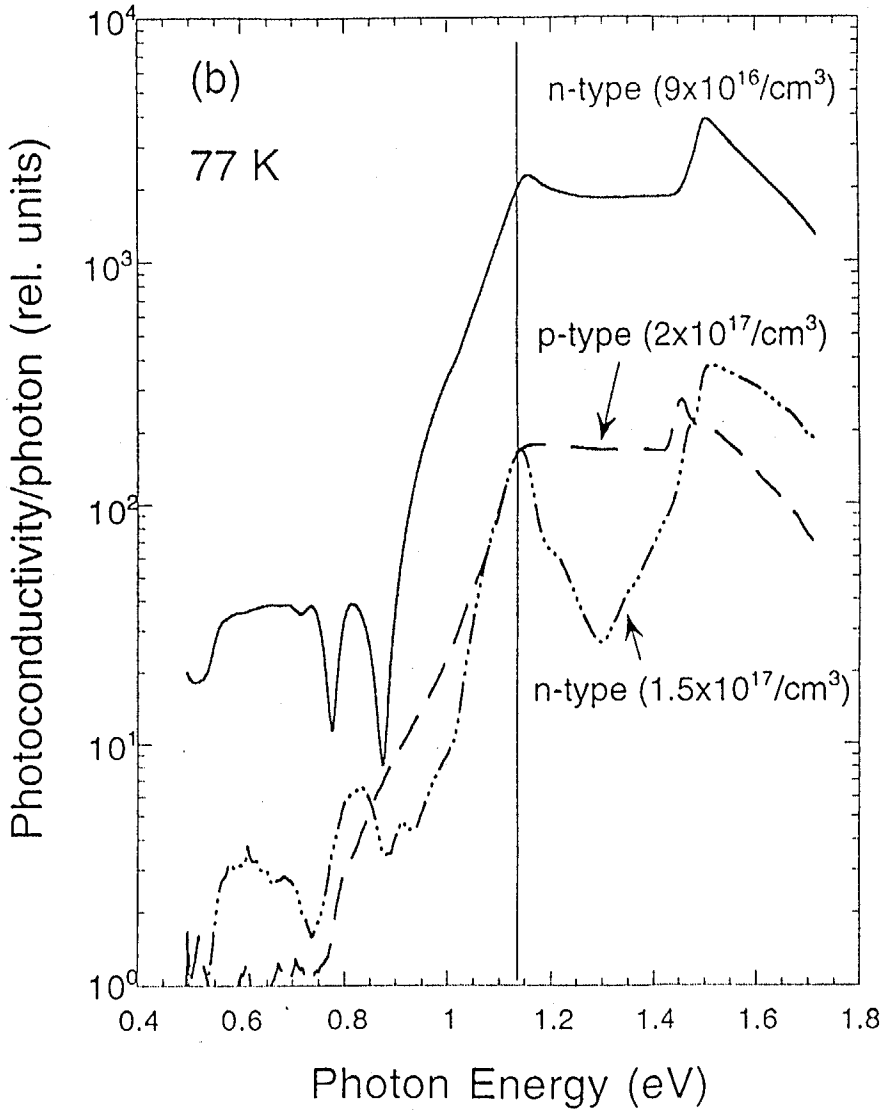
(b)
77 K
n-type (9x10^16/cm^3)
p-type (2x10^17/cm^3)
n-type (1.5x10^17/cm^3)
Photoconductivity/photon (rel. units)
Photon Energy (eV)
10^4
10^3
10^2
10^1
10^0
0.4
0.6
0.8
1
1.2
1.4
1.6
1.8